Dalton Transactions

PAPER

View Article Online
View Journal

Published on 18 June 2015. Downloaded by North Dakota State University on 08/07/2015 12:34:50.

Cite this: DOI: 10.1039/c5dt01564b

Palladium(0)-mediated C–H bond activation of *N*-(naphthyl)salicylaldimine and related ligands: utilization of the resulting organopalladium complexes in catalytic C–C and C–N coupling reactions†

Jayita Dutta,[a] Michael G. Richmond[b] and Samaresh Bhattacharya*[a]

Received 25th April 2015,
Accepted 9th June 2015

DOI: 10.1039/c5dt01564b

www.rsc.org/dalton

N-(Naphthyl)-4-R-salicylaldimines (R = OCH_3, H and Cl; H_2L^1–H_2L^3) and 2-hydroxy-*N*-(naphthyl)-naphthaldimine (H_2L^4) readily undergo, upon reaction with $Na_2[PdCl_4]$ in the presence of triphenylphosphine, cyclopalladation *via* C–H bond activation at the *peri*-position to afford complexes of type $[Pd(L)(PPh_3)]$ (L = L^1–L^4). The C–H bond activation has been found to be mediated by palladium(0) formed *in situ*. A similar reaction of H_2L^1 with $Na_2[PdCl_4]$ in the presence of 1,2-bis(diphenylphosphino)-ethane (dppe), in a 2 : 2 : 1 mole ratio, yields a dinuclear complex of type $[\{Pd(L^1)\}_2(dppe)]$. Reaction of H_2L^1 with $Na_2[PdCl_4]$ in the presence of 4-picoline (pic) yields $[Pd(L^1)(pic)]$. The molecular structures of the six complexes have been determined by X-ray crystallography. The aldiminate ligand in each compound is coordinated to the metal center as a di-anionic tridentate ONC-donor, with the fourth coordination site occupied by a phosphine or picoline ligand. The new complexes show intense absorptions in the visible and ultraviolet regions, and the nature of the optical transitions has been analyzed by TDDFT calculations. The palladium complexes display notable efficiency in catalyzing C–C and C–N bond coupling reactions. The thermodynamics for the formation of the cyclometalated catalyst precursor $[Pd(L^2)(PPh_3)]$ has been evaluated by DFT calculations.

Introduction

The chemistry of palladium complexes continues to receive considerable current attention,[1] largely because of the catalytic efficiency of palladium-based systems in a wide variety of industrially important reactions. Particularly notable are those reactions involving palladium-catalyzed carbon–carbon and carbon–heteroatom bond formations, which have emerged as some of the most powerful methods in the toolbox of synthetic organic chemists for the construction of valued heterocycles and commodity chemicals.[2] Given the importance of such reactions, coupled with our interest in this general area of catalysis, we have initiated a program dedicated to the synthesis and study of new organometallic precursors that are able to catalyze industrially important reactions.[3]

In the case of palladium-catalyzed C–C and C–heteroatom bond forming reactions, relatively stable palladium starting materials [*e.g.*, $PdCl_4^{2-}$, $PdCl_2$, $Pd_2(DBA)_3$] are typically employed as starting reagents for the generation of at least one highly reactive organo-palladium species that possesses a Pd–C bond during autogenous catalysis. Such labile species help account for the high turnover numbers typically exemplified by such reactions. Studies on the Pd–C bonded species, with particular reference to their formation and reactivity, help to strengthen our understanding of such useful catalytic intermediates and are therefore of significant contemporary importance. Our interest in this area of research centers on the synthesis of new palladium-based systems that contain a pincer ligand based on an aldiminate platform. Such

[a]*Department of Chemistry, Inorganic Chemistry Section, Jadavpur University, Kolkata 700 032, India. E-mail: samaresh_b@yahoo.com; Fax: +91-33-24146223*
[b]*Department of Chemistry, University of North Texas, Denton, TX 76203, USA*

† Electronic supplementary information (ESI) available: Selected bond lengths (Å) and angles (°) for $[Pd(L)(PPh_3)]$ (L = L^2, L^3 and L^4) (Table S1), results of TDDFT calculations on $[Pd(L)(PPh_3)]$ (L = L^2, L^3 and L^4) and $[Pd(L^1)(pic)]$ (Tables S2–S5), compositions of selected molecular orbitals of $[Pd(L)(PMe_3)]$ (L = L^2–L^4) and $[Pd(L^1)(pic)]$ (Tables S6–S9), C–C and C–N coupling using $Pd(OAc)_2$ and PPh_3 (Tables S10 and S11), crystallographic data for $[Pd(L)(PPh_3)]$ (L = L^2, L^3 and L^4) (Table S12), structures of $[Pd(L)(PPh_3)]$ (L = L^2, L^3 and L^4) (Fig. S1–S3), alternative mechanism of formation of cyclopalladated species (Scheme S1), contour plots of all molecular orbitals of $[Pd(L)(PMe_3)]$ (L = L^2–L^4) and $[Pd(L^1)(pic)]$ associated with the spectral transitions (Fig. S4–S7). CCDC 965740–965745. For ESI and crystallographic data in CIF or other electronic format see DOI: 10.1039/c5dt01564b

Published on 18 June 2015. Downloaded by North Dakota State University on 08/07/2015 12:34:50.

compounds have the potential to serve as novel precursors for preparation of reactive palladium catalysts in a wide variety of popular catalytic transformations.

The four Schiff bases, *viz*. three *N*-(naphthyl)-4-R-salicylaldimines (R = OCH_3, H and Cl; H_2L^1–H_2L^3) and 2-hydroxy-*N*-(naphthyl)naphthaldimine (H_2L^4), have been chosen as the principal ligands for the present study. The initial goal has been to induce an ONC-mode of binding (**I** and **II**) from these ligands, which requires the formal loss of two protons from the uncoordinated aldimine ligand – the phenolic proton and the naphthyl proton at the *peri*-position. The selected ligands are abbreviated in general as H_2L, and the H_2 portion of the formula represents the two hydrogens that are activated upon coordination of the aldimine ligand at the palladium center. The reaction of the selected aldimine ligands (H_2L^1–H_2L^4) with $Na_2[PdCl_4]$ is expected to furnish the corresponding cyclopalladated complexes containing the chelate motif **I** or **II**. The coordinatively unsaturated tricoordinated PdL chelates (**I** for L = L^1–L^3 and **II** for L = L^4) have been trapped by added donor ligands to yield the four-coordinate cyclopalladated products having the general formula [Pd(L)(L′)] (where L′ = PPh_3, 4-picoline, dppe). Herein we report our data on the synthesis of these new [Pd(L)(L′)] complexes, along with their characterization by a combination of spectroscopic methods, and X-ray diffraction analyses. DFT and TDDFT calculations have been conducted, and the ability of the cyclopalladated species to serve as precursors in catalytic C–C and C–N bond formation reactions is discussed.

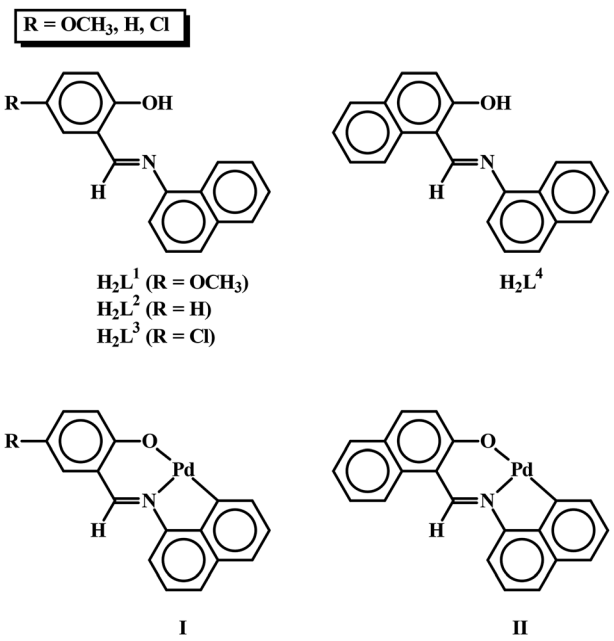

Results and discussion

Syntheses and structures

As outlined in the Introduction, the primary goal of this study was to explore the synthesis of a new family of cyclopalladated species *via* activation of the C–H bond at the *peri*-position of the *N*-naphthyl ring in the aldimine ligands (H_2L^1–H_2L^4) upon reaction with $Na_2[PdCl_4]$ in the presence of triphenylphosphine as the ancillary ligand. The planned reactions proceeded smoothly in refluxing ethanol in the presence of triethylamine, and from each of these reactions a yellow complex was obtained in a good yield. Preliminary characterization (microanalysis, NMR and IR) of the isolated products supports the expected composition, *viz*. a doubly de-protonated aldimine ligand and a triphenylphosphine coordinated to palladium, consistent with the general formula [Pd(L)-(PPh_3)] (L = L^1–L^4). The coordination mode exhibited by the aldiminate ligand in [Pd(L^1)(PPh_3)] was established by X-ray crystallography, and the structure is shown in Fig. 1. Selected bond parameters for [Pd(L^1)(PPh_3)] are listed in Table 1. The molecular structure confirms that the aldiminate ligand is indeed coordinated to the palladium center in the targeted ONC-fashion (**I**, R = OCH_3), forming two adjacent six- and five-membered chelate rings with bite angles of 90.67(8)° and 82.95(9)°, respectively. The coordinated triphenylphosphine ligand is situated *trans* to the imine-nitrogen of the aldiminate ligand, and the palladium is nested in a CNOP core of atoms that is distorted significantly from an idealized square-planar geometry, as manifested in the bond parameters around the metal center. The Pd–C, Pd–N, Pd–O and Pd–P bond distances are normal and compare well with those bond distances that are reported in structurally related palladium complexes.[4]

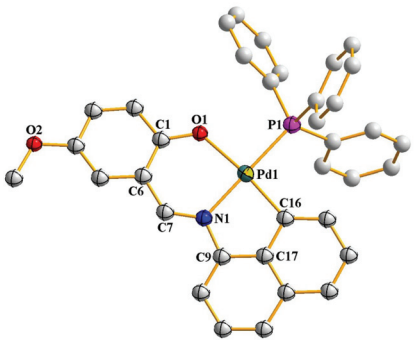

Fig. 1 Structure of [Pd(L^1)(PPh_3)].

The structures of the remaining three products were also established by X-ray diffraction analyses. Each compound displays an identical ONC-coordination of the aldiminate ligand to the palladium center, and the PPh_3 ligand occupies the remaining coordination site *trans* to the nitrogen atom of the activated aldimine ligand. Given the structural similarities between these compounds and [Pd(L^1)(PPh_3)], we have deposited these structures in the ESI (Fig. S1–S3 and Table S1†). It is relevant to mention here that the ONC-mode of coordination displayed by four aldiminate ligands in [Pd(L)(PPh_3)] (where L = L^1–L^4) represents a rare bonding mode in four-coordinate palladium(II) compounds.[5] Typically, such aldimine

This journal is © The Royal Society of Chemistry 2015

Published on 18 June 2015. Downloaded by North Dakota State University on 08/07/2015 12:34:50.

Table 1 Selected bond distances and bond angles for $[Pd(L^1)(PPh_3)]$, $[\{Pd(L^1)\}_2(dppe)]$ and $[Pd(L^1)(pic)]$

$[Pd(L^1)(PPh_3)]$			
Bond distances (Å)			
Pd1–O1	2.0516(17)	C1–O1	1.301(3)
Pd1–N1	2.043(2)	C7–N1	1.294(3)
Pd1–C16	2.007(2)	C9–N1	1.420(3)
Pd1–P1	2.2706(7)		
Bond angles (°)			
N1–Pd1–P1	179.27(6)	O1–Pd1–N1	90.67(8)
O1–Pd1–C16	173.49(9)	N1–Pd1–C16	82.95(9)
$[\{Pd(L^1)\}_2(dppe)]$			
Bond distances (Å)			
Pd1–O1	2.0700(14)	P1–C131	1.833(2)
Pd1–N1	2.0376(18)	C131–C131A	1.518(3)
Pd1–C16	1.992(2)	C1–O1	1.301(3)
Pd1–P1	2.2598(6)	C7–N1	1.288(3)
		C9–N1	1.426(3)
Bond angles (°)			
N1–Pd1–P1	176.50(5)	O1–Pd1–N1	91.20(7)
O1–Pd1–C16	174.03(8)	N1–Pd1–C16	82.99(8)
$[Pd(L^1)(pic)]$			
Bond distances (Å)			
Pd1–O1	2.061(3)	C1–O1	1.294(6)
Pd1–N1	1.992(3)	C7–N1	1.308(6)
Pd1–C16	1.976(3)	C9–N1	1.414(6)
Pd1–N2	2.051(3)		
Bond angles (°)			
N1–Pd1–N2	176.66(13)	O1–Pd1–N1	93.04(13)
O1–Pd1–C16	174.99(14)	N1–Pd1–C16	83.10(16)

ligands undergo reaction with transition metals to furnish the more common ON-mode of coordination.[6]

The formation of the cyclopalladated $[Pd(L)(PPh_3)]$ complexes was initially thought to occur *via* stepwise displacement of chloride ligands in $[PdCl_4]^{2-}$ by the aldimine ligand to give the monoanionic ON-chelated complex *cis*-$[PdCl_2(ON)]^-$. Ensuing substitution of one chloride by PPh_3, followed by cyclometalation *via* the formal elimination of HCl from the Pd-bound chloride and the naphthyl *peri*-proton would account for the observed products (Scheme S1, ESI†). While the reaction proceeds without problems in the presence of EtOH and Et_3N, no cyclopalladated product is observed in the absence of either of these reagents. This suggests that the role of Et_3N is more complex than simply serving as a scavenger of HCl in the last step of this mechanism. More probable is the *in situ* reduction of Pd(II) to Pd(0) by EtOH, in a Wacker-type reaction that is assisted by Et_3N. The involvement of palladium(0) was thus tested by repeating the reaction using a known precursor of palladium(0), *viz.* $[Pd_2(DBA)_3]$. Some speculated, but logical, sequences behind the palladium(0)-mediated formation of the cyclopalladated $[Pd(L)(PPh_3)]$ complexes are illustrated in Scheme 1 for the reaction between $[PdCl_4]^{2-}$ and H_2L^2. Here the initial step en route to cyclopalladation is believed to involve palladium coordination of both the aldimine and PPh_3 ligands to give the two-coordinate species **D**. Coordination of the aldimine ligand through the nitrogen moiety positions the phenolic O–H group in close proximity to the palladium, and this facilitates the oxidative addition of the O–H bond, which in turn gives the corresponding hydride complex **E**. Isomerization of **E** to **F** allows the PPh_3 ligand to reduce its unfavorable close contacts with the adjacent naphthyl appendage. Activation of the *peri* C–H bond of the naphthyl ligand, coupled with the loss of molecular hydrogen completes the reaction. In support of this process, we note that reactions between the aldimine ligands (H_2L) and $[Pd_2(DBA)_3]$ proceed smoothly in EtOH solvent in the presence of PPh_3. More importantly, no Et_3N is required and the isolated yield of the same $[Pd(L)(PPh_3)]$ product in each reaction is comparable to those reactions employing $Na_2[PdCl_4]$. We also examined the direct reaction of the aldimine ligands (H_2L) with $[Pd(PPh_3)_2Cl_2]$ but failed to obtain any tractable product, presumably due to kinetic reasons.

The thermodynamics for the conversion of the aldimine ligand H_2L^2 with palladium(0) to the corresponding product $[Pd(L^2)(PPh_3)]$ was investigated computationally by Density Functional Theory (DFT). The optimized structures and ground-state energy ordering for the pertinent species are depicted in Fig. 2. The reaction of palladium(0) (**A**), PPh_3 (**B**), and the aldimine H_2L^2 (**C**) gives the two-coordinate complex $Pd(H_2L^2)(PPh_3)$ (**D**). The ancillary ligands exhibit a near linear disposition and reveal a bond angle of *ca.* 172° for the N–Pd–P atoms. The formation of **D** is exergonic and the reaction lies 40.6 kcal mol^{-1} below the reagents (see Fig. 2). Activation of the pendant phenolic O–H bond affords the sterically congested four-coordinate hydride **E** that lies 6.1 kcal mol^{-1} lower in energy than **D**. Species **E** rearranges to the thermodynamically more stable hydride **F**. The **E** → **F** isomerization is promoted by a relief of unfavorable close contacts between the PPh_3 ligand and the naphthyl moiety in the former species. The naphthyl ring in **F** displays the needed geometry for *peri* C–H activation, which in turn is followed by the formation of the cyclopalladated species **G** and release of H_2 (**H**). The net thermodynamics are computed at −49.7 kcal mol^{-1} and are in agreement with the easily prepared and readily isolable nature of the cyclopalladated compounds described here.

The facile formation of the $[Pd(L)(PPh_3)]$ complexes prompted us to explore the synthesis of a dinuclear organopalladium complex using a bidentate diphosphine ligand instead of triphenylphosphine. Accordingly, 1,2-bis(diphenylphosphino)ethane (dppe) was chosen as the ligating diphosphine. The reaction of $Na_2[PdCl_4]$ with H_2L^1 and dppe in a 2 : 2 : 1 molar ratio in refluxing ethanol in the presence of triethylamine was successful and afforded an orange complex of the targeted nature, *viz.* $[\{Pd(L^1)\}_2(dppe)]$, in good yield. The coordination of two palladium centers by the dppe ligand in the isolated product was authenticated by single-crystal X-ray diffraction analysis. The molecular structure of $[\{Pd(L^1)\}_2(dppe)]$ is shown in Fig. 3, where each palladium center reveals a ONC-coordinated aldiminate ligand and the presence of the bridging dppe ligand. The metrical parameters for the bond distances and angles for the ligands about each palladium are unexceptional to those data found in the monophosphine

Published on 18 June 2015. Downloaded by North Dakota State University on 08/07/2015 12:34:50.

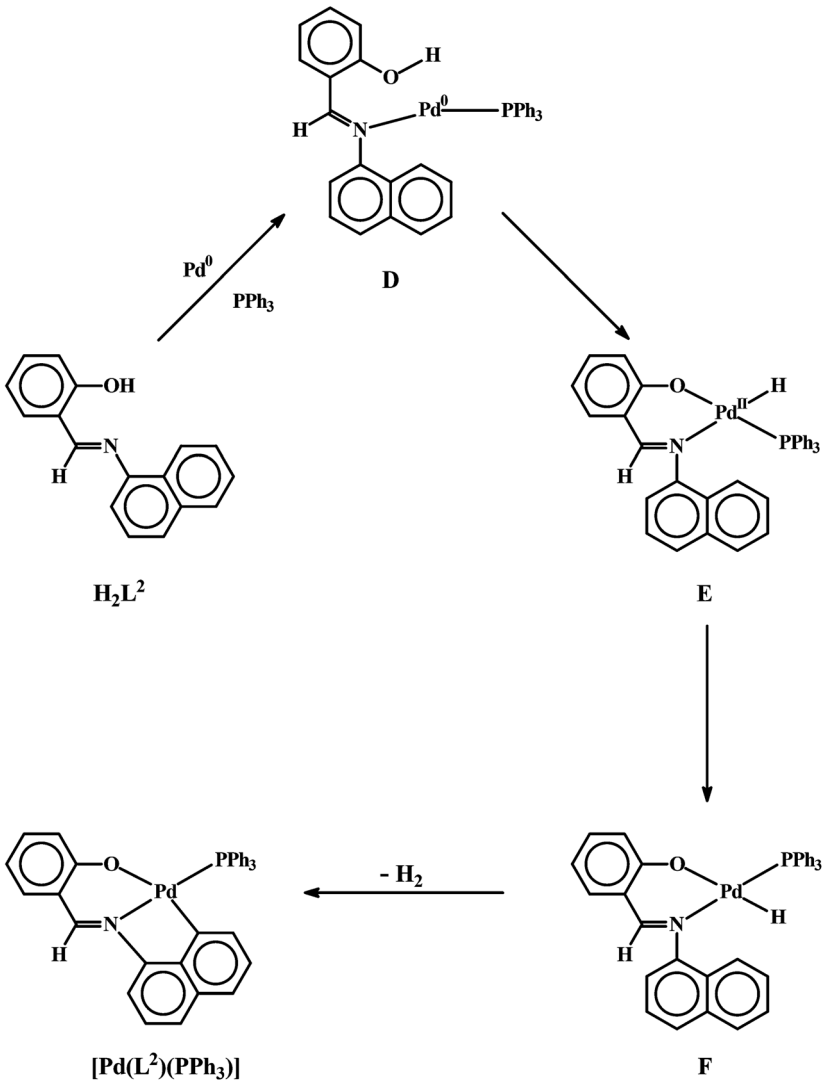

Scheme 1 Probable steps involved in the formation of the cyclopalladated complexes.

$[Pd(L)(PPh_3)]$ complexes already described here (Tables 1 and S1†).

The successful palladium-mediated C–H activation of the naphthyl moiety in the aldimine ligands (H_2L^1–H_2L^4), and the trapping of the resulting ONC-ligated Pd(L) fragment by phosphines, prompted us to check the feasibility of donor atoms other than phosphorus to trap the Pd(L) fragment in our reactions. To this end, we investigated the trapping of $Pd(L^1)$, formed from the reaction of $Na_2[PdCl_4]$ with H_2L^1, by 4-picoline (pic) under experimental conditions similar to those employed in the PPh_3 reactions. The product was isolated as an orange solid and its ^1H NMR spectrum was consistent with the expected composition, *viz.* $[Pd(L^1)(pic)]$. The molecular structure of $[Pd(L^1)(pic)]$ (Fig. 4) confirms the general course of the reaction and the ligation of 4-picoline at the fourth coordination site on palladium. The Pd(1)–N(picoline) bond distance is unexceptionable relative to other Pd–N(pyridine) distances,[7] and the bond parameters in the $Pd(L^1)$ fragment compare well with those found in Pd(L) fragments in our other structurally characterized complexes reported here (Tables 1 and S1†). We conclude that, like phosphines, coordination by a pyridine–nitrogen is also effective in stabilizing the $Pd(L^1)$ fragment.

Spectral properties

The ^1H, ^{13}C, and ^{31}P NMR spectra of these new complexes were recorded in $CDCl_3$ solution, and the NMR data are presented in the Experimental section. The ^1H NMR spectra of these complexes all displayed relatively narrow linewidths in keeping with their diamagnetic character. In $[Pd(L^1)(PPh_3)]$, $[\{Pd(L^1)\}_2(dppe)]$, and $[Pd(L^1)(pic)]$, the signal for the methoxy group in the aldiminate ligand is observed near 3.80 ppm. The azomethine proton signal was observed as a distinct downfield singlet at 9.50 and 8.79 ppm in $[Pd(L^4)(PPh_3)]$ and $[Pd(L^1)$-(pic)], respectively. This same resonance in the remaining four complexes was shifted upfield and obscured by overlapping

 This journal is © The Royal Society of Chemistry 2015

Published on 18 June 2015. Downloaded by North Dakota State University on 08/07/2015 12:34:50.

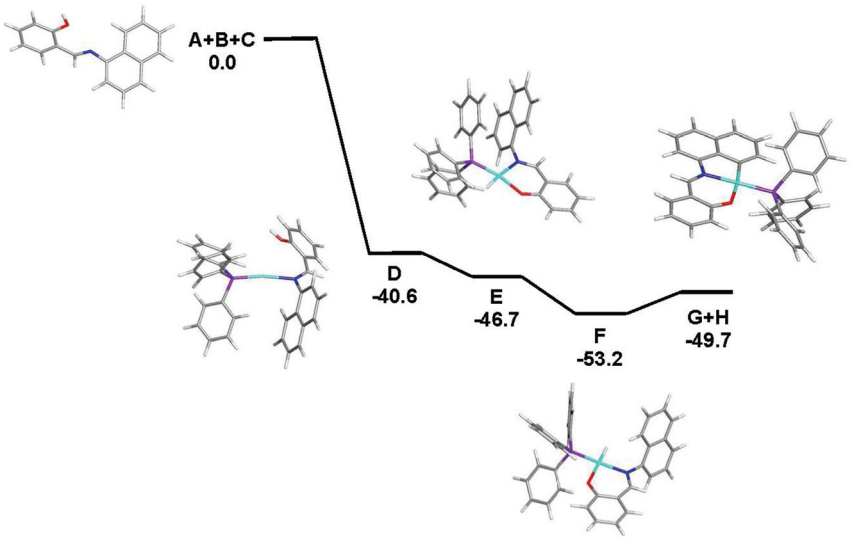

Fig. 2 B3LYP-optimized structures and ground-state energy ordering for the reaction of Pd(0) (**A**), PPh_3 (**B**), and H_2L^2 (**C**) to give the cyclopalladated complex $[Pd(L^2)(PPh_3)]$ (**G**) and H_2 (**H**). The free energy values are referenced relative to the reagents **A** + **B** + **C**. The optimized structures for **A**, **B**, and **H** are not shown.

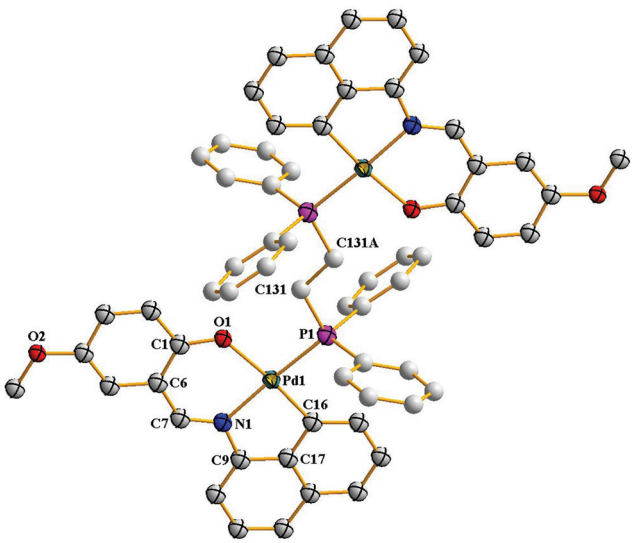

Fig. 3 Structure of $[\{Pd(L^1)\}_2(dppe)]$.

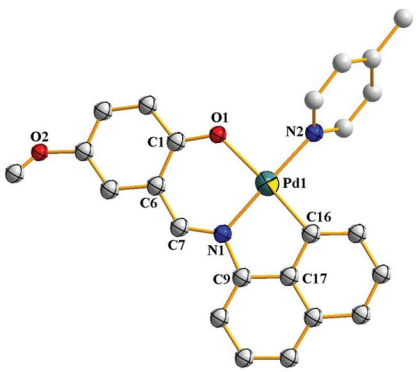

Fig. 4 Structure of $[Pd(L^1)(pic)]$.

aryl hydrogens. In the ^1H NMR spectrum of $[Pd(L^1)(pic)]$, the picoline ligand exhibits a singlet at 2.49 ppm for the methyl group and two doublets at 7.32 and 8.89 ppm for the pairwise equivalent pyridyl hydrogens. The ^{31}P NMR spectra recorded for the different $[Pd(L)(PPh_3)]$ complexes (L = L^1–L^4) reveal a single resonance within 43.0–44.8 ppm for the coordinated phosphine. In $[\{Pd(L^1)\}_2(dppe)]$, a single ^{31}P resonance appears at 35.3 ppm consistent with a structure whose palladium centers exhibit a similar coordination environment. The ^{13}C NMR spectra of the $[Pd(L)(PPh_3)]$ (L = L^1–L^4), $[Pd(L^1)(pic)]$ and $[\{Pd(L^1)\}_2(dppe)]$ complexes show all the expected signals for the coordinated ligands, and these data are summarized in the Experimental section.

The infrared spectra of all the complexes show many bands of varying intensities within 4000–450 cm^{-1}. While a detailed spectral assignment has not been attempted due to the complexity, we can confidently assign the moderately strong ν(C=N) stretch *ca.* 1600 cm^{-1} in each complex to the imine moiety of the aldiminate ligand.[8] All six products display a phenolic C–O stretching band *ca.* 1100 cm^{-1}. The NMR and infrared spectral data of the complexes are therefore consistent with their compositions.

These new palladium complexes are readily soluble in acetone, dichloromethane, chloroform, and acetonitrile, producing intense yellow solutions. We have recorded the electronic spectra of these complexes in dichloromethane solution, and the UV-vis spectral data are presented in Table 2. Each complex shows several intense absorptions over the

Published on 18 June 2015. Downloaded by North Dakota State University on 08/07/2015 12:34:50.

Table 2 Electronic spectral data of the complexes in dichloromethane solution

Complex	λ_{max}, nm (ε, M^{-1} cm^{-1})
[Pd(L^1)(PPh_3)]	494 (4680), 404[a] (4000), 384[a] (4980), 298[a] (9930)
[Pd(L^2)(PPh_3)]	460 (5310), 398[a] (4630), 376[a] (5000), 292[a] (11 650)
[Pd(L^3)(PPh_3)]	468 (8480), 404[a] (7020), 382[a] (7150), 294[a] (17 820)
[Pd(L^4)(PPh_3)]	480 (9420), 454 (9770), 384[a] (12 840), 318[a] (13 300)
[{Pd(L^1)}$_2$(dppe)]	498 (5080), 412[a] (3850), 388[a] (4760), 300[a] (8710), 270[a] (13 030)
[Pd(L^1)(pic)]	496 (6550), 412[a] (5460), 392[a] (6210), 270[a] (15 370)

[a] Shoulder.

range 800–200 nm. To provide insight into the nature of these absorptions, TDDFT calculations have been performed on all four [Pd(L)(PPh_3)] (L = L^1–L^4) complexes and [Pd(L^1)(pic)], using the Gaussian 03 program package.[9] In the [Pd(L)(PPh_3)] (L = L^1–L^4) complexes, the phenyl rings of the triphenylphosphine have been replaced by methyl groups in order to simplify the calculations.[10] The computational results from the TDDFT calculations are similar for all four [Pd(L)(PMe_3)] (L = L^1–L^4) complexes and [Pd(L^1)(pic)], and hence only the results for [Pd(L^1)(PMe_3)] are given in Table 3; the data for the other three [Pd(L)(PMe_3)] (L = L^2–L^4) complexes and [Pd(L^1)-(pic)] are summarized in Tables S2–S5 (ESI†). Fig. 5 shows the contour plots of selected molecular orbitals of [Pd(L^1)(PMe_3)], while Table 4 contains the orbital assignments for the electronic spectral transitions computed for [Pd(L^1)(PMe_3)]. The corresponding orbital and electronic transition data for the remaining PPh_3- and picoline-substituted complexes may be found in Tables S6–S9 and Fig. S4–S7 (ESI†). Since the computed orbital and optical transition data are qualitatively similar for this genre of compounds, only the complex [Pd(L^1)-(PMe_3)] will be discussed in detail here. The lowest energy absorption at 494 nm is attributable to a combination of HOMO → LUMO and HOMO−1 → LUMO transitions, and based on the nature of the participating orbitals, the electronic excitation is assignable largely to an intra-ligand charge-transfer (ILCT) transition, with a minor metal-to-ligand charge-transfer (MLCT) and ligand-to-metal charge transfer (LMCT) character. The next two lower energy absorptions at 404 and 384 nm exhibit similar orbital parentage. The absorption band at 298 nm is primarily due to a HOMO−2 → LUMO+2 transition that is best described as having a MLCT character, where the HOMO−2 has a significantly large metal contribution and the LUMO+2 is delocalized mostly over the aldiminate ligand.

Catalytic activity

Given the superior activity reported for numerous palladium complexes in C–C and C–N bond cross coupling reactions,[11] we next explored the catalytic efficacy of our complexes in Suzuki-type C–C bond cross-coupling and Buchwald-type C–N bond cross-coupling reactions.

We began our study with the Suzuki coupling of phenylboronic acid and *p*-iodoacetophenone, using [Pd(L^1)(PPh_3)] as the catalyst, to yield the biphenyl product. After extensive optimization, it was found that 0.001 mol% catalyst, 1.7 equiv. of NaOH as the base, polyethyleneglycol as the solvent, and 2 h at 120 °C furnished the desired C–C coupled product in quantitative yield (Table 5, entry 1). The other three [Pd(L)-(PPh_3)] (L = L^2–L^4) complexes displayed comparable catalytic activity under similar reaction conditions (entries 2–4). [{Pd(L^1)}$_2$(dppe)] also efficiently catalyzed the same coupling reaction; however, compared to [Pd(L^1)(PPh_3)], significantly (50%) less reaction time was needed for the former to achieve 100% yield of the product (entry 5), a fact we attribute to the two-fold increase in palladium concentration in the di-palladium complex. With [Pd(L^1)(pic)] as the catalyst, a slightly longer time was required to achieve quantitative conversion to the 4-phenylacetophenone product (entry 6).

The Suzuki coupling of other aryl halides with phenylboronic acid was next examined. Since the four [Pd(L)(PPh_3)] (L = L^1–L^4) complexes show similar catalytic efficiencies (entries 1–4), we limited these studies to the catalyst precursors [Pd(L^2)-

Table 3 Computed parameters from TDDFT calculations on [Pd(L^1)(PMe_3)] for electronic spectral properties in dichloromethane solution

Transition number	Nature of transition	CI value	E/eV	Oscillator strength, f	λ_{theo}/nm	Assignment
1	H−1 → L	−0.10940	2.6530	0.1297	467.34 (494)[a]	ILCT/LMCT/MLCT
	H → L	0.64904				ILCT/LMCT/MLCT
2	H−1 → L	0.66346	3.1256	0.2974	396.68 (404)[a]	ILCT/LMCT/MLCT
3	H−3 → L	0.11398	3.8480	0.0226	322.20 (384)[a]	ILCT/LMCT/MLCT
	H → L+1	0.64084				ILCT/LMCT/MLCT
	H → L+2	0.18189				ILCT/LMCT/MLCT
4	H−6 → L	−0.18118	4.2480	0.0609	291.87 (298)[a]	ILCT/LMCT/MLCT
	H−2 → L+2	0.49738				ILCT/LLCT/LMCT/MLCT
	H−1 → L+1	0.28170				ILCT/LMCT/MLCT
	H−1 → L+2	0.17581				ILCT/LLCT/LMCT/MLCT
	H−1 → L+3	0.11773				ILCT/MLCT

[a] λ_{exp}/nm is given in parenthesis.

This journal is © The Royal Society of Chemistry 2015

Published on 18 June 2015. Downloaded by North Dakota State University on 08/07/2015 12:34:50.

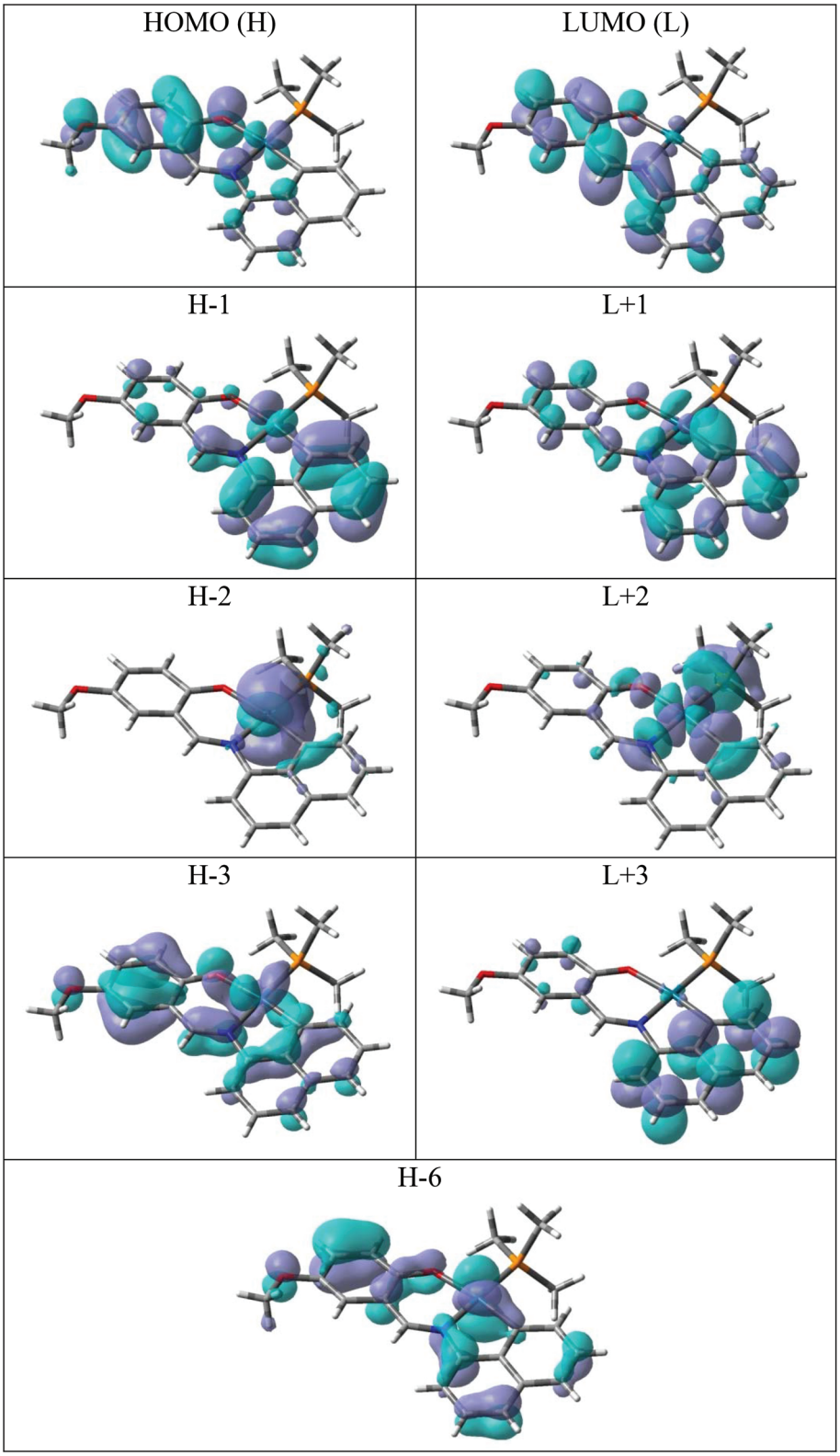

Fig. 5 Contour plots of the molecular orbitals of [Pd(L^1)(PMe_3)], which are associated with the electronic spectral transitions (see Table 3).

(PPh_3)], [{Pd(L^1)}$_2$(dppe)], and [Pd(L^1)(pic)]. The coupling of phenylboronic acid with *p*-iodobenzaldehyde and *p*-iodobenzonitrile, which are more electron deficient than *p*-iodoacetophenone, using [Pd(L^2)(PPh_3)] furnished the expected biaryls in 100% yield, but these reactions proceeded slower, requiring 3 h for completion (entries 7 and 8). A similar trend was

Published on 18 June 2015. Downloaded by North Dakota State University on 08/07/2015 12:34:50.

Table 4 Compositions of all molecular orbitals of [Pd(L^1)(PMe_3)] associated with the electronic spectral transitions

Molecular orbital	% Contribution of fragments		
	Pd	L^1	PMe_3
L+3	4.7	95.3	0
L+2	16.4	64.6	19.0
L+1	11.1	88.9	0
L	9.5	90.5	0
H	13.2	86.8	0
H−1	13.5	86.5	0
H−2	56.8	29.0	14.2
H−3	16.4	83.6	0
H−6	15.1	84.9	0

observed with the aryl bromides (entries 9–13), with longer reaction times necessary to achieve comparable reaction yields. The observed turnover numbers for coupling with these aryl iodides, as well as aryl bromides, are extremely high ($\sim 10^5$) and compare favorably to the high turnover numbers reported in other palladium-based catalytic systems.[12] The use of *p*-chloroacetophenone as a substrate led to lower turnover numbers, coupled with a much higher catalyst loading and longer reaction times (entries 14–16). The variation in yield, upon changing the substituent from $-COCH_3$ to –CHO to –CN in the aryl chloride, was quite significant (entries 14, 17 and 18). Coupling of phenylboronic acid was also studied with 2-bromopyridine, and for proper comparison we have also examined bromobenzene as a substrate (entries 19–23). Inclusion of nitrogen in the aryl ring was found to impede the coupling reaction, as manifested in longer reaction times needed for 2-bromopyridine compared to bromobenzene (entries 19–21).

The observed ease of the Suzuki coupling reactions, with particular reference to the mild reaction conditions, low catalyst loading, and high yields, prompted us to investigate the catalytic activity of these complexes in Buchwald-type C–N bond coupling reactions of halobenzenes with primary and secondary amines. The C–N bond coupling of iodobenzene with three primary aromatic amines was initially attempted using [Pd(L^2)(PPh_3)] as the catalyst. The reactions were found to proceed smoothly with 0.01 mol% catalyst, 1.7 equiv. of NaO^tBu as the base, polyethyleneglycol as the solvent, 145 °C reaction temperature, XPhos as the additive, and 15 h reaction time, to afford the expected products in good yield (Table 6, entries 1–3). The catalytic efficiency of the same complex towards C–N bond coupling involving iodobenzene and the secondary amines piperidine and morpholine proceeds in an analogous fashion (entries 4 and 5). Replacement of iodobenzene by bromobenzene requires higher catalyst loadings (10×) and longer reaction times to achieve full conversion to the corresponding product (entries 6–10). C–N bond coupling involving aryl chloride substrates could only be achieved in moderate yields with longer reaction times and much higher (1.0 mol%) catalyst loadings (entries 11–15). In order to assess the effectiveness of our catalysts, some selected C–C and C–N coupling reactions were also carried out using a traditional catalyst, *viz*. $Pd(OAc)_2$ and PPh_3, and the results are presented in Tables S10 and S11 (ESI†). While efficiency of the traditional catalyst was found to be comparable with that of the cyclopalladated species for the C–C coupling reactions, the C–N coupling reactions were unsuccessful with the traditional catalyst even for iodobenzene substrate.

The palladium complexes are thus found to be efficient catalysts for C–C and C–N bond coupling reactions. It is interesting to note that for the Suzuki coupling reactions, which involved relatively low catalyst loadings and afforded the coupled product in reasonably high yield, no additional ligand was necessary. This indicates that the organic ligands coordinated to palladium in the native catalyst do not dissociate during *in situ* generation of the palladium(0) necessary for the catalysis, and they adequately stabilize the reduced metal center. A plausible mechanism for the observed catalytic C–C cross-coupling reactions is presented in Scheme 2. In the initial step, the palladium(II) center in the pre-catalyst undergoes a two-electron reduction to generate a palladium(0) species **[1]**, where the N-bound aldimine ligand (H_2L) is believed to remain coordinated to the reduced metal center, along with the triphenylphosphine. The following steps that lead to the intermediates **[2]**, **[3]**, and **[4]** are all usual for such coupling reactions, and these are followed by formation of the coupled product and regeneration of the active catalyst **[1]**. Another interesting aspect of this observed Suzuki reactions is that the catalysts not only activate aryl–I and aryl–Br bonds, but can also activate the notoriously difficult aryl–Cl bond and afford C–C bond coupled products in 100% yield. Documented catalysts capable of activating aryl–Cl bonds efficiently are scarce in the literature.[13] The observed catalytic efficiency of the present group of complexes is superior in comparison to other known molecular palladium complexes under similar ligand-free conditions.[14] The electronic nature of the substituents in the aldimine ligand has no measureable influence on the catalytic activities of these complexes.

Notwithstanding the higher catalyst loadings needed in the C–N bond coupling reactions, compared to the Suzuki C–C bond couplings (Table 5), the Buchwald-type couplings reported here are facile, an atypical trait in contrast to the majority of reported catalytic studies.[11b–d,f] Drawing from the published work of Barder and Buchwald,[15] we propose the mechanism in Scheme 3 for our observed C–N bond coupling reactions. Here the *in situ* generation of palladium(0) is believed to take place in the initial step, with simultaneous loss of the coordinated aldimine ligand. The XPhos ligand, which serves to stabilize the reduced metal center, was found to be essential for the catalysis to proceed smoothly. The remaining steps are the usual ones for such C–N coupling reactions. The catalytic efficiency of the present group of Pd(II) complexes in C–N bond coupling reactions is comparable to that of several other palladium complexes under similar experimental conditions.[16]

This journal is © The Royal Society of Chemistry 2015

Published on 18 June 2015. Downloaded by North Dakota State University on 08/07/2015 12:34:50.

Table 5 Suzuki cross-coupling of aryl halides with phenylboronic acids[a]

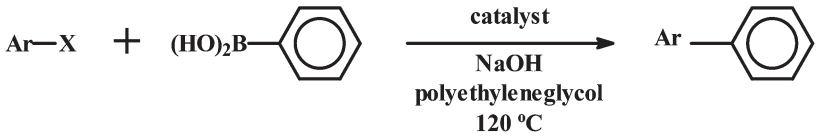

Entry	Aryl halide	Catalyst	Time (h)	Amt of cat. (mol%)	Yield[b] (%)	TON
1	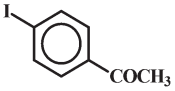	[Pd(L^1)(PPh$_3$)]	2	0.001	100	100 000
2	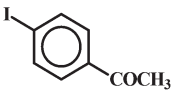	[Pd(L^2)(PPh$_3$)]	2	0.001	100 (89)[c]	100 000
3	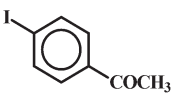	[Pd(L^3)(PPh$_3$)]	2	0.001	100	100 000
4	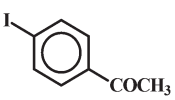	[Pd(L^4)(PPh$_3$)]	2	0.001	100	100 000
5	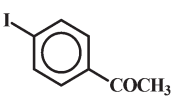	[{Pd(L^1)}$_2$(dppe)]	1	0.001	100	100 000
6	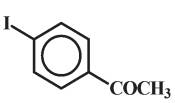	[Pd(L^1)(pic)]	3	0.001	100	100 000
7	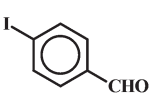	[Pd(L^2)(PPh$_3$)]	3	0.001	100 (84)[c]	100 000
8	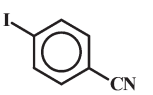	[Pd(L^2)(PPh$_3$)]	3	0.001	98 (83)[c]	98 000
9	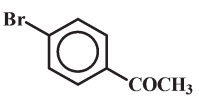	[Pd(L^2)(PPh$_3$)]	6	0.001	100 (82)[c]	100 000
10	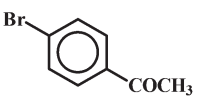	[{Pd(L^1)}$_2$(dppe)]	4	0.001	100	100 000
11	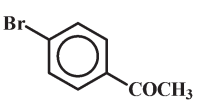	[Pd(L^1)(pic)]	8	0.001	100	100 000
12	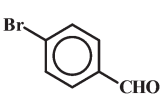	[Pd(L^2)(PPh$_3$)]	8	0.001	100 (79)[c]	100 000
13	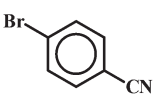	[Pd(L^2)(PPh$_3$)]	8	0.001	100 (80)[c]	100 000
14	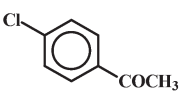	[Pd(L^2)(PPh$_3$)]	24	0.01	100 (83)[c]	10 000

Published on 18 June 2015. Downloaded by North Dakota State University on 08/07/2015 12:34:50.

Table 5 *(Contd.)*

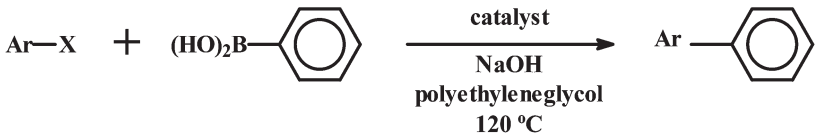

Entry	Aryl halide	Catalyst	Time (h)	Amt of cat. (mol%)	Yield[b] (%)	TON
15	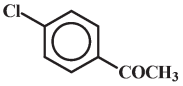	[{Pd(L^1)}$_2$(dppe)]	20	0.01	100	10 000
16	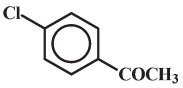	[Pd(L^1)(pic)]	24	0.01	75	7500
17	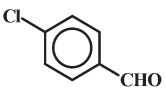	[Pd(L^2)(PPh$_3$)]	24	0.01	34 (27)[c]	3400
18	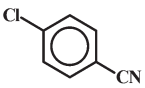	[Pd(L^2)(PPh$_3$)]	24	0.01	18 (14)[c]	1800
19	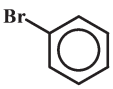	[Pd(L^2)(PPh$_3$)]	5	0.001	100 (85)[c]	100 000
20	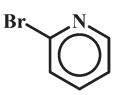	[Pd(L^2)(PPh$_3$)]	5	0.001	67	67 000
21	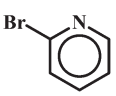	[Pd(L^2)(PPh$_3$)]	8	0.001	100 (78)[c]	100 000
22	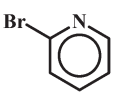	[Pd(L^1)(dppe)]	7	0.001	100	100 000
23	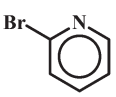	[Pd(L^1)(pic)]	8	0.001	82	82 000

[a] Reaction conditions: aryl halide (1.0 mmol), phenylboronic acid (1.2 mmol), NaOH (1.7 mmol), Pd catalyst, polyethyleneglycol (4 mL). [b] Determined by GCMS. [c] Isolated yield.

Conclusions

The present study shows that the *N*-(naphthyl)salicylaldimine-based ligands (H_2L^1–H_2L^4) readily undergo, upon reaction with $Na_2[PdCl_4]$ in the presence of triphenylphosphine, cyclopalladation *via* C–H bond activation at the *peri*-position to afford complexes of type [Pd(L)(PPh$_3$)] (L = L^1–L^4). Cyclopalladation is also achieved using 1,2-bis(diphenylphosphino) ethane or 4-picoline as an ancillary ligand. All of the cyclopalladated complexes are found to be convenient catalyst precursors for highly efficient Suzuki-type C–C and Buchwald-type C–N bond coupling reactions.

Experimental

Material and measurements

Palladium chloride was obtained from Arora Matthey, Kolkata, India. $Na_2[PdCl_4]$ was prepared by following a reported procedure.[17] 1-Naphthylamine was purchased from Loba Chemie, Mumbai, India, while the salicylaldehyde, 2-hydroxynaphthaldehyde, and triphenylphosphine used in these studies were purchased from Spectrochem, Mumbai, India. 5-Methoxysalicylaldehyde and 5-chlorosalicylaldehyde were procured from Alfa Aesar, and 1,2-bis(diphenylphosphino)ethane (dppe) was purchased from Sigma-Aldrich. The Schiff bases (H_2L^1–H_2L^4)

 This journal is © The Royal Society of Chemistry 2015

Published on 18 June 2015. Downloaded by North Dakota State University on 08/07/2015 12:34:50.

Table 6 C–N cross-coupling reaction of aryl halides with amines[a]

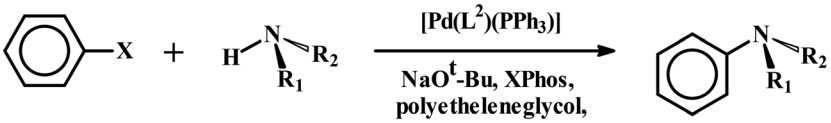

Entry	X	Amine	Amt of cat. (mol%)	Time (h)	Yield[b] (%)	TON
1	I	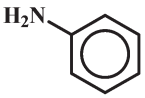	0.01	15	100 (89)[c]	10 000
2	I	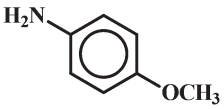	0.01	15	100 (83)[c]	10 000
3	I	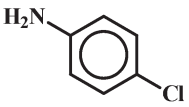	0.01	15	100 (84)[c]	10 000
4	I		0.01	15	100 (85)[c]	10 000
5	I	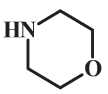	0.01	15	100 (87)[c]	10 000
6	Br	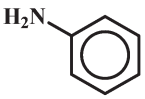	0.1	20	100 (81)[c]	1000
7	Br	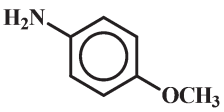	0.1	20	100	1000
8	Br	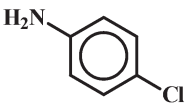	0.1	20	100	1000
9	Br		0.1	20	100 (86)[c]	1000
10	Br	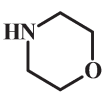	0.1	20	100	1000
11	Cl	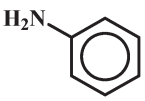	1.0	24	55 (47)[c]	55
12	Cl	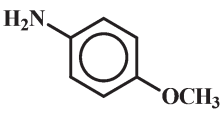	1.0	24	50	50

Published on 18 June 2015. Downloaded by North Dakota State University on 08/07/2015 12:34:50.

Table 6 *(Contd.)*

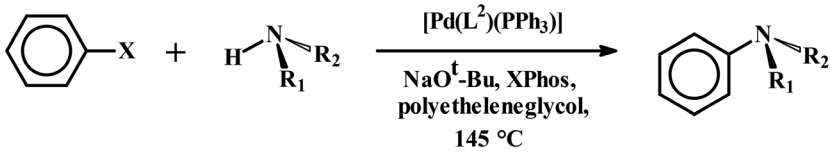

Entry	X	Amine	Amt of cat. (mol%)	Time (h)	Yield[b] (%)	TON
13	Cl	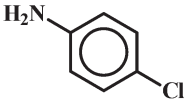	1.0	24	60	60
14	Cl		1.0	24	45 (38)[c]	45
15	Cl	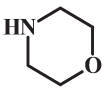	1.0	24	47	47

[a] Reaction conditions: aryl halide (1.0 mmol), amines (1.0 mmol), NaO^t-Bu (1.7 mmol), Pd catalyst, polyethyleneglycol (4 mL), XPhos (0.1 mmol). [b] Determined by GCMS. [c] Isolated yield.

were prepared by refluxing equimolar amounts of 1-naphthylamine and the respective aldehyde in absolute ethanol. All other chemicals and solvents were reagent grade commercial materials and were used as received. Microanalyses (C, H, and N) were performed using a Heraeus Carlo Erba 1108 elemental analyzer. NMR spectra were recorded in $CDCl_3$ solution on a Bruker Avance DPX 300 NMR spectrometer. IR spectra were recorded on a Perkin Elmer Spectrum Two IR spectrometer, with samples prepared as KBr pellets. Electronic spectra were recorded on a JASCO V-570 spectrophotometer. GC-MS analyses were performed using a Perkin Elmer CLARUS 680 instrument.

Preparation of the complexes

The [Pd(L)(PPh_3)] (L = L^1–L^4) complexes were prepared by following a general procedure. Specific details are given below for the H_2L^1-derived complex.

[Pd(L^1)(PPh_3)]. To a solution of H_2L^1 (47 mg, 0.17 mmol) in hot ethanol (20 mL) was added triethylamine (34 mg, 0.34 mmol), followed by a solution of $Na_2[PdCl_4]$ (50 mg, 0.17 mmol) in ethanol (10 mL). The solution was heated at reflux for 10 min and then triphenylphosphine (45 mg, 0.17 mmol) was added to the reaction mixture. Stirring at reflux was continued for an additional 6 h, yielding a yellow solution. The solvent was evaporated and the solid mass, thus obtained, was subjected to purification by thin-layer chromatography on a silica plate. With 1 : 1 hexane–benzene as the eluent, a yellow band separated, which was extracted with acetonitrile. Upon evaporation of the acetonitrile extract, [Pd(L^1)(PPh_3)] was obtained as a crystalline yellow solid (yield 62%).[18] ^{1}H NMR (300 MHz, $CDCl_3$):[19] δ (ppm) = 3.76 (s, OCH_3), 6.17 (d, J = 9.0 Hz, 1H), 6.66 (t, J = 7.5 Hz, 1H), 6.75 (d, J = 3.0 Hz, 1H), 6.79 (t, J = 7.5 Hz, 1H), 6.89 (dd, J = 3.0 Hz, 1H), 7.37–7.86 (PPh_3 + 4H)*, 8.99 (d, J = 12.0 Hz, 1H). ^{13}C NMR (500 MHz, $CDCl_3$): δ (ppm) = 56.1, 108.3, 113.8, 121.1, 122.3, 123.1, 124.8, 125.9, 126.7, 127.8, 128.0, 130.5, 134.1, 134.7, 135.2, 135.7, 135.9, 150.7, 151.4, 153.2, 154.1 and 168.6. ^{31}P NMR (500 MHz, $CDCl_3$): δ (ppm) = 43.04. IR (KBr, cm^{-1}): 3429, 3051, 2918, 1736, 1638, 1593, 1551, 1520, 1455, 1436, 1410, 1354, 1235, 1212, 1099, 1045, 949, 833, 810, 767, 752, 692, 569, 532, 514 and 497. $C_{36}H_{28}NO_2PPd$: calcd C: 67.08; H: 4.35; N: 2.17; found C: 67.11; H: 4.33; N: 2.19%.

[Pd(L^2)(PPh_3)]. Yield 65%. ^{1}H NMR (300 MHz, $CDCl_3$): δ (ppm) = 6.21 (d, J = 9.0 Hz, 1H), 6.48 (t, J = 7.5 Hz, 1H), 6.65 (t, J = 6.0 Hz, 1H), 6.78 (t, J = 7.5 Hz, 1H), 7.15 (t, J = 9.0 Hz, 1H), 7.34–7.86 (PPh_3 + 5H)*, 9.03 (d, J = 15.0 Hz, 1H). ^{13}C NMR (500 MHz, $CDCl_3$): δ (ppm) = 108.9, 114.1, 120.7, 122.9, 123.4, 125.2, 126.2, 127.2, 128.1, 128.2, 130.8, 134.2, 134.7, 135.1, 135.8, 135.9, 150.3, 151.1, 153.7, 154.5 and 169.9. ^{31}P NMR (500 MHz, $CDCl_3$): δ (ppm) = 43.03. IR (KBr, cm^{-1}): 3467, 3049, 1605, 1554, 1515, 1480, 1438, 1386, 1359, 1234, 1196, 1147, 1129, 1098, 1028, 999, 927, 853, 811, 752, 692, 556, 532, 515 and 497. $C_{35}H_{26}NOPPd$: calcd C: 68.41; H: 4.23; N: 2.28; found C: 68.43; H: 4.20; N: 2.29%.

[Pd(L^3)(PPh_3)]. Yield 61%. ^{1}H NMR (300 MHz, $CDCl_3$): δ (ppm) = 6.12 (d, J = 9.0 Hz, 1H), 6.66 (t, J = 6.0 Hz, 1H), 6.79 (t, J = 7.5 Hz, 1H), 7.05 (dd, J = 9.0 Hz, 1H), 7.31 (d, J = 3.0 Hz, 1H), 7.37–7.89 (PPh_3 + 4H)*, 8.94 (d, J = 12.0 Hz, 1H). ^{13}C NMR (500 MHz, $CDCl_3$): δ (ppm) = 109.6, 116.2, 121.2, 123.1, 124.5, 126.4, 126.9, 127.8, 128.4, 129.0, 132.2, 134.5, 134.9, 135.3, 135.6, 136.1, 150.5, 151.7, 153.8, 156.3 and 169.6. ^{31}P NMR (500 MHz, $CDCl_3$): δ (ppm) = 43.10. IR (KBr, cm^{-1}): 3436, 3053,

 This journal is © The Royal Society of Chemistry 2015

Published on 18 June 2015. Downloaded by North Dakota State University on 08/07/2015 12:34:50.

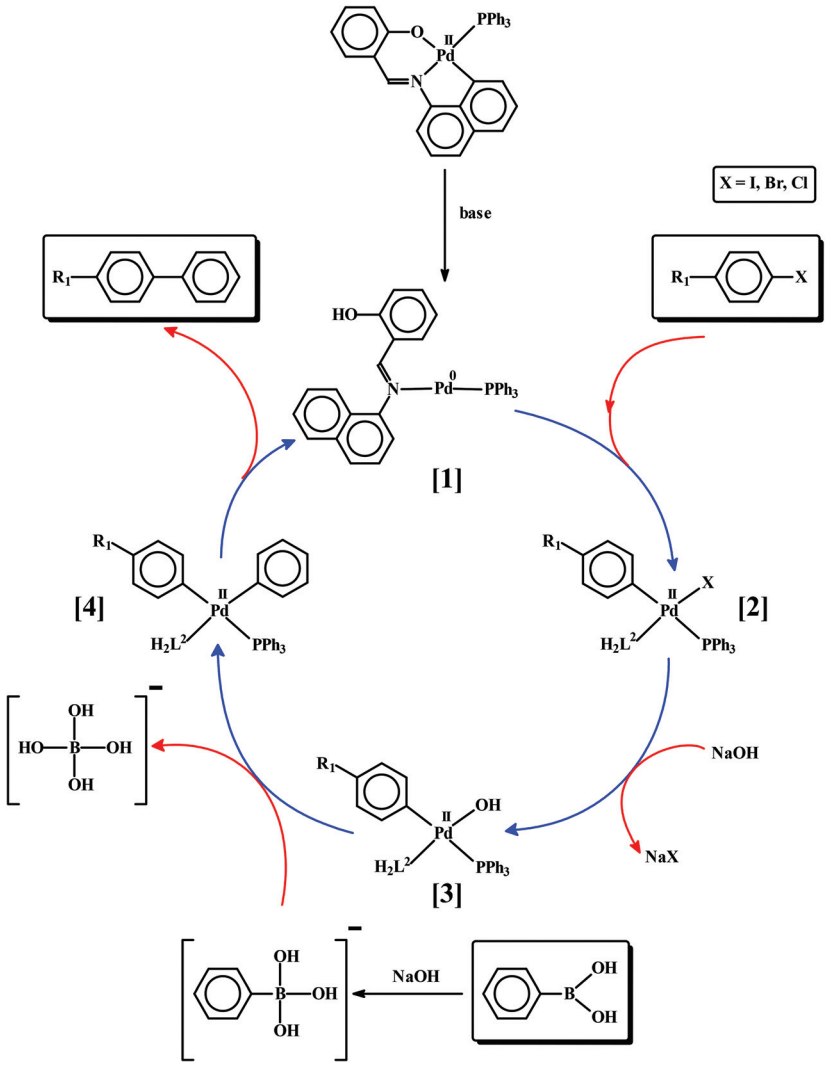

Scheme 2 Probable mechanism for the observed C–C cross-coupling reactions. H_2L^2 in **[2]**, **[3]** and **[4]** represents the N-coordinated aldimine ligand in **[1]**.

1607, 1552, 1508, 1480, 1446, 1436, 1415, 1386, 1361, 1232, 1190, 1157, 1098, 1026, 998, 829, 811, 765, 754, 692, 658, 565, 532, 514 and 498. $C_{35}H_{25}NOPClPd$: calcd C: 64.77; H: 3.85; N: 2.16; found C: 64.79; H: 3.82; N: 2.19%.

[Pd(L^4)(PPh$_3$)]. Yield 68%. ^{1}H NMR (300 MHz, $CDCl_3$): δ (ppm) = 6.33 (d, J = 12.0 Hz, 1H), 6.69 (t, J = 6.0 Hz, 1H), 6.82 (t, J = 7.5 Hz, 1H), 7.21 (d, J = 3.0 Hz, 1H), 7.36–7.93 (PPh_3 + 5H)*, 8.20 (d, J = 9.0 Hz, 1H), 8.36 (t, J = 4.5 Hz, 1H), 9.50 (s, azomethine), 10.04 (d, J = 15.0 Hz, 1H). ^{13}C NMR (500 MHz, $CDCl_3$): δ (ppm) = 109.7, 111.1, 114.4, 118.6, 119.2, 121.5, 123.0, 123.8, 126.1, 126.9, 127.7, 127.9, 128.2, 128.3, 129.5, 131.2, 133.3, 134.3, 135.1, 136.5, 144.1, 157.3, 166.5, 168.1 and 169.4. ^{31}P NMR (500 MHz, $CDCl_3$): δ (ppm) = 44.78. IR (KBr, cm^{-1}): 3436, 1620, 1566, 1450, 1399, 1349, 1313, 1212, 1159, 1138, 1084, 1035, 827, 768, 746, 594 and 565. $C_{39}H_{28}NOPPd$: calcd C: 70.48; H: 4.22; N: 2.11; found C: 70.51; H: 4.21; N: 2.13%.

The [Pd(L)(PPh$_3$)] (L = L^1–L^4) complexes could also be prepared using [Pd$_2$(DBA)$_3$] as the source of palladium. Since the experimental conditions employed in this alternative procedure are similar for all of the reactions examined, only the details for the synthesis of [Pd(L^1)(PPh$_3$)] are reported.

[Pd(L^1)(PPh$_3$)]. To a solution of H_2L^1 (31 mg, 0.11 mmol) in hot ethanol (30 mL) was added [Pd$_2$(DBA)$_3$] (50 mg, 0.05 mmol). The solution was heated at reflux for 10 min, and then triphenylphosphine (29 mg, 0.11 mmol) was added to the reaction mixture. The mixture was heated at reflux for 6 h to yield a yellow solution. The solvent was evaporated and the solid mass, thus obtained, was subjected to purification by thin-layer chromatography on a silica plate. With 1 : 1 hexane–benzene as the eluent, a yellow band separated, which was extracted with acetonitrile. Upon evaporation of the acetonitrile extract, [Pd(L^1)(PPh$_3$)] was obtained as a crystalline yellow solid (yield 55%).[20]

Published on 18 June 2015. Downloaded by North Dakota State University on 08/07/2015 12:34:50.

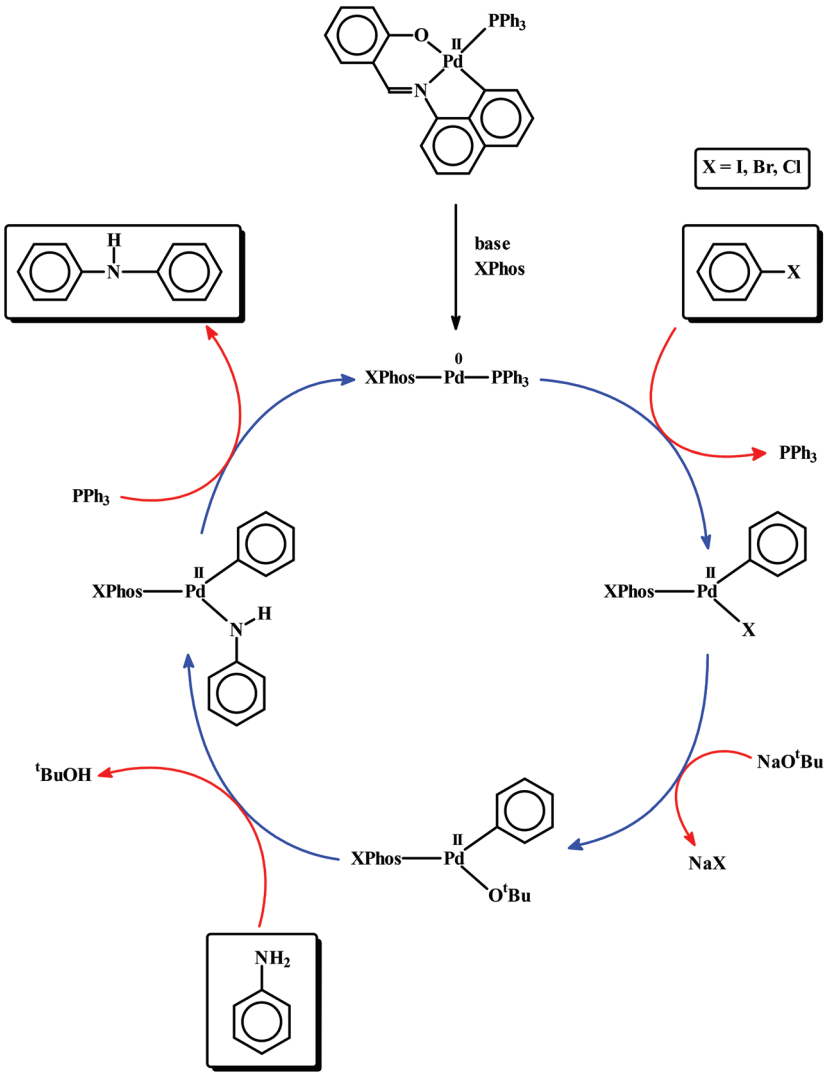

Scheme 3 Probable mechanism for the observed C–N coupling reactions.

[{Pd(L^1)}$_2$(dppe)]. To a solution of H_2L^1 (47 mg, 0.17 mmol) in hot ethanol (20 mL) triethylamine (34 mg, 0.34 mmol) was added followed by a solution of $Na_2[PdCl_4]$ (50 mg, 0.17 mmol) in ethanol (10 mL). The mixture was heated at reflux for 10 min, then 1,2-bis(diphenylphosphino)ethane (34 mg, 0.085 mmol) was added to the reaction mixture, and the reflux was continued for 6 h. [{Pd(L^1)}$_2$(dppe)] started to precipitate as an orange crystalline solid during the reflux. The reaction solution was allowed to cool to room temperature, and the desired product was then collected by filtration, washed thoroughly with water, followed by ethanol, and then dried in air (yield 75%). ^{1}H NMR (300 MHz, $CDCl_3$): δ (ppm) = 1.56 (s, 4H), 3.77 (s, 2OCH$_3$), 6.22 (d, J = 6.0 Hz, 2H), 6.62 (d, J = 9.0 Hz, 2H), 6.71 (t, J = 7.5 Hz, 2H), 7.31–7.78 (2PPh$_2$ + 12H)*, 8.97 (t, J = 4.5 Hz, 2H). ^{13}C NMR (500 MHz, $CDCl_3$): δ (ppm) = 28.8, 56.3, 108.4, 113.6, 121.0, 122.3, 123.2, 124.8, 125.7, 126.8, 127.6, 128.4, 129.7, 134.0, 134.6, 135.1, 135.5, 137.4, 150.6, 151.3, 153.1, 154.2 and 168.7. ^{31}P NMR (500 MHz, $CDCl_3$): δ (ppm) = 35.26. IR (KBr, cm^{-1}): 3437, 3036, 1600, 1554, 1524, 1455, 1436, 1419, 1403, 1371, 1316, 1260, 1237, 1215, 1194, 1156, 1116, 1101, 1082, 1039, 999, 922, 808, 760, 747, 694, 676, 568, 524 and 489. $C_{62}H_{50}N_2O_4P_2Pd_2$: calcd C: 64.04; H: 4.30; N: 2.41; found C: 64.07; H: 4.28; N: 2.42%.

[Pd(L^1)(pic)]. To a solution of H_2L^1 (47 mg, 0.17 mmol) in hot ethanol (20 mL) triethylamine (34 mg, 0.34 mmol) was added followed by a solution of $Na_2[PdCl_4]$ (50 mg, 0.17 mmol) in ethanol (10 mL). The mixture was heated at reflux for 10 min and 4-picoline (16 mg, 0.17 mmol) was then added to the reaction mixture. This was allowed to reflux for 6 h to yield an intense orange solution. The solvent was evaporated and the solid mass, thus obtained, was subjected to purification by thin-layer chromatography on a silica plate. With 1 : 20 acetonitrile-benzene as the eluent, an intense orange band separated, which was extracted with acetonitrile. Upon evaporation

This journal is © The Royal Society of Chemistry 2015

Published on 18 June 2015. Downloaded by North Dakota State University on 08/07/2015 12:34:50.

of the acetonitrile extract [Pd(L^1)(pic)] was obtained as a crystalline orange solid (yield 63%). ^{1}H NMR (300 MHz, $CDCl_3$): δ (ppm) = 2.49 (s, CH_3), 3.80 (s, OCH_3), 6.63 (d, J = 6.0 Hz, 1H), 6.80 (d, J = 3.0 Hz, 1H), 6.84 (s, 1H), 7.06 (dd, J = 9.0 Hz, 1H), 7.16 (t, J = 7.5 Hz, 1H), 7.32 (d, J = 6.0 Hz, 2H), 7.43 (t, J = 7.5 Hz, 1H), 7.50 (d, J = 9.0 Hz, 1H), 7.61 (d, J = 9.0 Hz, 1H), 7.73 (d, J = 9.0 Hz, 1H), 8.79 (s, 1H), 8.89 (d, J = 6.0 Hz, 2H). ^{13}C NMR (500 MHz, $CDCl_3$): δ (ppm) = 21.42, 56.23, 109.03, 111.84, 114.90, 119.04, 122.81, 124.47, 125.49, 126.18, 126.52, 126.76, 129.90, 133.74, 140.62, 148.78, 150.09, 152.01, 152.82, 153.82, 159.65 and 165.24. IR (KBr, cm^{-1}): 3436, 3045, 2927, 1600, 1556, 1523, 1459, 1438, 1411, 1391, 1308, 1262, 1215, 1156, 1080, 1040, 927, 809, 768, 743, 556 and 508. $C_{24}H_{20}N_2O_2Pd$: calcd C: 60.14; H: 4.17; N: 5.85; found C: 60.16; H: 4.14; N: 5.88%.

X-ray crystallography

Single crystals of [Pd(L)(PPh_3)] (L = L^1–L^4), [{Pd(L^1)}$_2$(dppe)] and [Pd(L^1)(pic)] were obtained by slow evaporation of solvent from solutions of the respective complexes in acetonitrile. Selected crystal data and data collection parameters for [Pd(L^1)(PPh_3)], [{Pd(L^1)}$_2$(dppe)] and [Pd(L^1)(pic)] are given in Table 7, and those for [Pd(L)(PPh_3)] (L = L^2–L^4) are given in Table S12 (ESI†). Data on all the crystals were collected on a Bruker SMART CCD diffractometer. X-ray data reduction, structure solution and refinement were performed using the SHELXS-97 and SHELXL-97 packages.[21] The structures were solved by direct methods.

Computational modeling and TDDFT calculations

Geometry optimization by the density functional theory (DFT) method and electronic spectral analysis for the TDDFT calculations were performed using the Gaussian 03 (B3LYP/SDD-6-31G) package.[9] The different species in Scheme 1 were examined computationally using Morokuma's ONIOM method using the Gaussian 09 software suite.[22] The PPh_3 and all species containing the coordinated phosphine were optimized *via* a two-level approach, with the phenyl groups of the PPh_3 treated as the lower of the two levels; all other compounds depicted in the scheme were optimized by *ab initio* DFT methods. For those species analyzed within the two-level treatment, we employed an ONIOM method that was defined by a B3LPY/PM6 composition. The phenyl groups (low level) were treated at the semiempirical PM6 level of theory, while the remaining atoms (high level) were treated within the B3LYP framework. With respect to the high-level treatment of atoms, the palladium atoms were described with the Stuttgart–Dresden effective core potential (ecp) and a SDD basis set, while a 6-31+G(d′) basis set was employed for the remaining atoms. All of the species in Scheme 1 furnished fully optimized ground-state structures based on positive eigenvalues obtained from the analytical Hessian. Unscaled vibrational frequencies were used to make zero-point and thermal corrections to the electronic energies.

Application as catalysts

General procedure for Suzuki coupling reactions. In a typical run, an oven-dried 10 mL round bottom flask was

Table 7 Crystallographic data for [Pd(L^1)(PPh_3)], [{Pd(L^1)}$_2$(dppe)] and [Pd(L^1)(pic)]

Complex	[Pd(L^1)(PPh_3)]	[{Pd(L^1)}$_2$(dppe)]	[Pd(L^1)(pic)]
Empirical formula	$C_{36}H_{28}NO_2PPd$	$C_{62}H_{50}N_2O_4P_2Pd_2$	$3(C_{24}H_{20}N_2O_2Pd)\cdot H_2O$
Formula weight	643.98	1161.82	1442.52
Crystal system	Monoclinic	Triclinic	Monoclinic
Space group	$P2_1/c$	$P\bar{1}$	$P2_1/c$
a/Å	15.6731(6)	8.6555(2)	14.3458(4)
b/Å	11.7347(4)	12.6136(3)	15.7571(5)
c/Å	17.4108(6)	13.6905(3)	26.8926(8)
α/°	90	104.844(1)	90
β/°	116.042(2)	107.335(1)	94.016(2)
γ/°	90	105.750(1)	90
V/Å^3	2877.07(18)	1277.47(5)	6064.1(3)
Z	4	1	4
D_{calcd}/mg m^{-3}	1.487	1.510	1.578
F(000)	1312	590	2912
λ/Å	0.71073	0.71073	0.71073
Crystal size/mm^3	0.14 × 0.18 × 0.26	0.15 × 0.15 × 0.18	0.25 × 0.25 × 0.26
Temp./K	296	273	296
μ/mm^{-1}	0.735	0.818	0.943
Collected reflections	44 600	21 569	102 218
R_{int}	0.040	0.026	0.033
Independent reflections	6244	5886	14 085
R_1[a]	0.0262	0.0246	0.0392
wR_2[b]	0.0850	0.0662	0.1196
GOF[c]	1.08	1.02	0.93

[a] $R_1 = \sum||F_o| - |F_c||/\sum|F_o|$. [b] $wR_2 = [\sum\{w(F_o^2 - F_c^2)^2\}/\sum\{w(F_o^2)\}]^{1/2}$. [c] GOF = $[\sum(w(F_o^2 - F_c^2)^2)/(M - N)]^{1/2}$, where M is the number of reflections and N is the number of parameters refined.

Published on 18 June 2015. Downloaded by North Dakota State University on 08/07/2015 12:34:50.

charged with a known mole percent of catalyst, NaOH (1.7 mmol), phenylboronic acid (1.2 mmol), aryl halide (1 mmol), and the appropriate solvents (4 mL). The flask was placed in a preheated oil bath at the required temperature. After the specified time had been reached, the flask was removed from the oil bath and water (20 mL) was added, followed by extraction with ether (4 × 10 mL). The combined organic layers were washed with water (3 × 10 mL), dried over anhydrous Na_2SO_4, and filtered. The solvent was removed under vacuum. The residue was dissolved in hexane and analyzed by GCMS. In selected cases the product was isolated *via* purification by thin-layer chromatography on a silica plate.

General procedure for C–N coupling reactions. In a typical run, an oven-dried 10 mL round bottom flask was charged with a known mole percent of catalyst, NaO^{t}Bu (1.7 mmol), XPhos (0.1 mmol), amine (1.0 mmol), aryl halide (1.0 mmol), and the appropriate solvent(s) (4 mL). The flask was placed in a preheated oil bath at the required temperature. After the specified time, the flask was removed from the oil bath, water (20 mL) was added, and extraction with ether (4 × 10 mL) was carried out. The combined organic layers were washed with water (3 × 10 mL), dried over anhydrous Na_2SO_4, and filtered. The solvent was removed under vacuum. The residue was dissolved in acetonitrile and analyzed by GCMS. In selected cases the product was isolated *via* purification by thin-layer chromatography on a silica plate.

Acknowledgements

We thank the referees for their constructive comments, which have been helpful in preparing the revised manuscript. Financial assistance received from the Department of Science and Technology, Government of West Bengal, Kolkata [Sanction No. 746(Sanc.)/ST/P/S&T/2G-4/2013)] is gratefully acknowledged. M.G.R. thanks the Robert A. Welch Foundation (grant B-1093) and acknowledges computational resources through UNT's High Performance Computing Services and CASCaM. Jayita Dutta thanks the Council of Scientific and Industrial Research, New Delhi, for her fellowship [Grant No. 09/096 (0702)/2011-EMR-I]. The authors thank Dr Debajyoti Ghoshal of JU for his help in sorting out some problems related to the refinement of a crystal structure.

References

1 (*a*) A. R. Kapdi and I. J. S. Fairlamb, *Chem. Soc. Rev.*, 2014, 4751–4777; (*b*) K. J. Bonney and F. Schoenebeck, *Chem. Soc. Rev.*, 2014, 6609–6638; (*c*) N. Cutillas, G. S. Yellol, C. Haro, C. Vicente, V. Rodriguez and J. Ruiz, *Coord. Chem. Rev.*, 2013, **257**, 2784–2797; (*d*) L. M. Mirica and J. R. Khusnutdinova, *Coord. Chem. Rev.*, 2013, **257**, 299–314; (*e*) T. Moriuchi and T. Hirao, *Acc. Chem. Res.*, 2012, **45**, 347–360; (*f*) N. B. Debata, D. Tripathy and D. K. Chand, *Coord. Chem. Rev.*, 2012, **256**, 1831–1945; (*g*) S. Komiya, *Coord. Chem. Rev.*, 2012, **256**, 556–573; (*h*) V. K. Jain and L. Jain, *Coord. Chem. Rev.*, 2010, **254**, 2848–2903; (*i*) D. B. D. Amico, L. Labella, F. Marchetti and S. Samaritani, *Coord. Chem. Rev.*, 2010, **254**, 635–645; (*j*) R. D. Adams and B. Captain, *Acc. Chem. Res.*, 2009, **42**, 409–418; (*k*) A. Garoufis, S. K. Hadjikakou and N. Hadjiliadis, *Coord. Chem. Rev.*, 2009, **253**, 1384–1397; (*l*) J. Vicente and A. Arcas, *Coord. Chem. Rev.*, 2005, **249**, 1135–1154; (*m*) L. Canovese, G. Chessa, F. Visentin and P. Uguagliati, *Coord. Chem. Rev.*, 2004, **248**, 945–954; (*n*) K. J. Szabo, *Chem. Soc. Rev.*, 2001, **30**, 136–143.

2 (*a*) J. L. Bras and J. Muzart, *Chem. Soc. Rev.*, 2014, **43**, 3003–3040; (*b*) S. T. Gadge and B. M. Bhanage, *RSC Adv.*, 2014, **4**, 10367–10389; (*c*) J. Ye and S. Ma, *Acc. Chem. Res.*, 2014, **47**, 989–1000; (*d*) A. Nakamura, T. M. J. Anselment, J. Claverie, B. Goodall, R. F. Jordan, S. Mecking, B. Rieger, A. Sen, P. W. N. M. Van Leeuwen and K. Nozaki, *Acc. Chem. Res.*, 2013, **46**, 1438–1449; (*e*) D. C. Powers and T. Ritter, *Acc. Chem. Res.*, 2012, **45**, 840–850; (*f*) L. Guo, X. Duan and Y. Liang, *Acc. Chem. Res.*, 2011, **44**, 111–122; (*g*) A. Molnar, *Chem. Rev.*, 2011, **111**, 2251–2320; (*h*) N. Selander and K. J. Szabo, *Chem. Rev.*, 2011, **111**, 2048–2076; (*i*) S. Cacchi and G. Fabrizi, *Chem. Rev.*, 2011, **111**, 215–283; (*j*) X. Wu, H. Neumann and M. Beller, *Chem. Soc. Rev.*, 2011, **40**, 4986–5009; (*k*) P. Sehnal, R. J. K. Taylor and I. J. S. Fairlamb, *Chem. Rev.*, 2010, **110**, 824–889; (*l*) G. P. Chiusoli, M. Catellani, M. Costa, E. Motti, N. D. Ca and G. Maestri, *Coord. Chem. Rev.*, 2010, **254**, 456–469; (*m*) C. A. Fleckensteinab and H. Plenio, *Chem. Soc. Rev.*, 2010, **39**, 694–711; (*n*) S. Wurtz and F. Glorius, *Acc. Chem. Res.*, 2008, **41**, 1523–1533; (*o*) L. Yin and J. Liebscher, *Chem. Rev.*, 2007, **107**, 133–173; (*p*) A. Roglans, A. Pla-Quintana and M. Moreno-Manas, *Chem. Rev.*, 2006, **106**, 4622–4643.

3 (*a*) J. Dutta and S. Bhattacharya, *RSC Adv.*, 2013, **3**, 10107–10721; (*b*) P. Majumder, P. Paul, P. Sengupta and S. Bhattacharya, *J. Organomet. Chem.*, 2013, **736**, 1–8; (*c*) P. Paul, P. Sengupta and S. Bhattacharya, *J. Organomet. Chem.*, 2013, **724**, 281–288; (*d*) J. Dutta, S. Datta, D. K. Seth and S. Bhattacharya, *RSC Adv.*, 2012, **2**, 11751–11763; (*e*) S. Datta, D. K. Seth, S. Halder, W. S. Sheldrick, H. Mayer-Figge, M. G. B. Drew and S. Bhattacharya, *RSC Adv.*, 2012, **2**, 5254–5264; (*f*) D. K. Seth, M. G. B. Drew and S. Bhattacharya, *J. Indian Chem. Soc.*, 2011, **88**, 1233–1240; (*g*) P. Paul, S. Datta, S. Halder, R. Acharyya, F. Basuli, R. J. Butcher, S. M. Peng, G. H. Lee, A. Castineiras, M. G. B. Drew and S. Bhattacharya, *J. Mol. Catal. A: Chem.*, 2011, **344**, 62–74.

4 (*a*) S. Guo and H. V. Huynh, *Organometallics*, 2014, **33**, 2004–2011; (*b*) M. Kalita, P. Gogoi, P. Barman, B. Sarma, A. K. Buragohain and R. D. Kalita, *Polyhedron*, 2014, **76**, 93–98; (*c*) W. X. C. Oliveira, M. M. da Costa, A. P. S. Fontes, C. B. Pinheiro, F. C. S. de Paula, E. H. L. Jaimes, E. F. Pedroso, P. P. de Souza, E. C. Pereira-Maia and C. L. M. Pereira, *Polyhedron*, 2014, **76**, 16–21; (*d*) N. Smrecki, B. Kukovec, J. Jazwinski, Y. Liu, J. Zhang,

 This journal is © The Royal Society of Chemistry 2015

Published on 18 June 2015. Downloaded by North Dakota State University on 08/07/2015 12:34:50.

A. Mikecin and Z. Popovic, *J. Organomet. Chem.*, 2014, **760**, 224–230; (*e*) K. R. Chaudhari, A. P. Wadawale, M. Kumar and V. K. Jain, *J. Organomet. Chem.*, 2014, **760**, 55–59.

5 J. Dutta, M. G. Richmond and S. Bhattacharya, *Eur. J. Inorg. Chem.*, 2014, 4600–4610.

6 (*a*) S. Liu, H. Sun, Y. Ma, S. Ye, X. Liu, X. Zhou, X. Mou, L. Wang, Q. Zhao and W. Huang, *J. Mater. Chem.*, 2012, **22**, 22167–22173; (*b*) G. H. Shahverdizadeh, S. W. Ng, E. R. T. Tiekink and B. Mirtamizdoust, *Acta Crystallogr., Sect. E: Struct. Rep. Online*, 2012, **68**, m278; (*c*) E. Safaei, M. M. Kabir, A. Wojtczak, Z. Jaglicic, A. Kozakiewicz and Y. Lee, *Inorg. Chim. Acta*, 2011, **366**, 275–282; (*d*) Z. Guo, L. Li, C. Wang, J. Li and T. Xu, *Acta Crystallogr., Sect. E: Struct. Rep. Online*, 2009, **65**, m1049; (*e*) Q. Zhao, L. Li, F. Li, M. Yu, Z. Liu, T. Yi and C. Huang, *Chem. Commun.*, 2008, 685–687; (*f*) Z. Liu, L. X. Jin, J. H. Xia and G. Z. Li, *Acta Crystallogr., Sect. E: Struct. Rep. Online*, 2007, **63**, m2488; (*g*) J. Dong, L. Li, L. Gao, T. Xu and D. Wang, *Acta Crystallogr., Sect. E: Struct. Rep. Online*, 2007, **63**, m1375–m1376; (*h*) L. Wang, J. Dong, L. Li, L. Li and D. Wang, *Acta Crystallogr., Sect. E: Struct. Rep. Online*, 2007, **63**, m1059–m1060; (*i*) W. Wang and G. Jin, *Inorg. Chem. Commun.*, 2005, **8**, 109–112.

7 S. Halder, S. M. Peng, G. H. Lee, T. Chatterjee, A. Mukherjee, S. Dutta, U. Sanyal and S. Bhattacharya, *New J. Chem.*, 2008, **32**, 105–114.

8 N. B. Colthup, L. H. Daly and S. E. Wiberley, *Introduction to Infrared and Raman Spectroscopy*, Academic Press, NY, 1990.

9 M. J. Frisch, G. W. Tracks, H. B. Schlegel, G. E. Scuseria, M. A. Robb, J. R. Cheeseman, J. A. Montgomery Jr., T. Vreven, K. N. Kudin, J. C. Burant, J. M. Millam, S. S. Iyengar, J. Tomasi, V. Barone, B. Mennucci, M. Cossi, G. Scalamani, N. Rega, G. A. Petersson, H. Nakatsuji, M. Hada, M. Ehara, K. Toyota, R. Fukuda, I. Hasegawa, M. Ishida, T. Nakajima, Y. Honda, O. Kitao, H. Nakai, M. Klene, X. Li, J. E. Knox, H. P. Hratchian, J. B. Cross, V. Bakken, C. Adamo, J. Jaramillo, R. Gomperts, R. E. Stratmann, O. Yazyev, A. J. Austin, R. Cammi, C. Pomelli, J. W. Ochterski, P. Y. Ayala, K. Morokuma, G. A. Voth, P. Salvador, J. J. Dannenberg, V. G. Zakrzewski, S. Dapprich, A. D. Daniels, M. C. Strain, O. Farkas, D. K. Malick, A. D. Rabuck, K. Raghavachari, J. B. Foresman, J. V. Ortiz, Q. Cui, A. G. Baboul, S. Clifford, J. Cioslowski, B. B. Stefanov, G. Liu, A. Liashenko, P. Piskroz, I. Komaromi, R. L. Martin, D. J. Fox, T. Keith, M. A. Al-Laham, C. Y. Peng, A. Nanayakkara, M. Challacombe, P. M. W. Gill, B. Johnson, W. Chen, M. W. Wong, C. Gonzalez and J. A. Pople, *GAUSSIAN 03 (Revision D01)*, Gaussian Inc., Pittsburgh, PA., 2003.

10 Partitioning [{Pd(L^1)}$_2$(dppe)] into two equal halves possessing a Ph_2PCH_2-ligand, gives [Pd(L^1)(PMe_3)] after the phenyl groups and the ethanol bridge carbon are replaced by methyl groups.

11 (*a*) A. Kumar, G. K. Rao, S. Kumar and A. K. Singh, *Dalton Trans.*, 2013, **42**, 5200–5223; (*b*) V. P. Boyarskiya, K. V. Luzyanina and V. Y. Kukushkin, *Coord. Chem. Rev.*, 2012, **256**, 2029–2056; (*c*) T. M. Shaikh, C. Weng and F. Hong, *Coord. Chem. Rev.*, 2012, **256**, 771–803; (*d*) V. Polshettiwar, C. Len and A. Fihri, *Coord. Chem. Rev.*, 2009, **253**, 2599–2626; (*e*) C. Barnard, *Platinum Met. Rev.*, 2008, **52**, 38–45; (*f*) A. Fihri, P. Meunier and J. C. Hierso, *Coord. Chem. Rev.*, 2007, **251**, 2017–2055; (*g*) E. M. Beccalli, G. Broggini, M. Martinelli and S. Sottocornola, *Chem. Rev.*, 2007, **107**, 5318–5365; (*h*) R. B. Bedford, C. S. J. Cazin and D. Holder, *Coord. Chem. Rev.*, 2004, **248**, 2283–2321; (*i*) K. Ferre-Filmon, L. Delaude, A. Demonceau and A. F. Noels, *Coord. Chem. Rev.*, 2004, **248**, 2323–2336; (*j*) C. J. Elsevier, *Coord. Chem. Rev.*, 1999, **185**, 809–822.

12 (*a*) M. Ghotbinejad, A. R. Khosropour, I. Mohammadpoor-Baltork, M. Moghadam, S. Tangestaninejad and V. Mirkhani, *J. Mol. Catal. A: Chem.*, 2014, **385**, 78–84; (*b*) Q. Wu, L. Wu, L. Zhang, H. Fu, X. Zheng, H. Chen and R. Li, *Tetrahedron*, 2014, **70**, 3471–3477; (*c*) P. Pattanayak, J. L. Pratihar, D. Patra, C. Lin and S. Chattopadhyay, *Polyhedron*, 2013, **63**, 133–138; (*d*) K. Wang, T. Yi, X. Yu, X. Zheng, H. Fu, H. Chen and R. Li, *Appl. Organomet. Chem.*, 2012, **26**, 342–346; (*e*) S. Li, Y. Lin, J. Cao and S. Zhang, *J. Org. Chem.*, 2007, **72**, 4067–4072; (*f*) J. H. Li and W. J. Liu, *Org. Lett.*, 2004, **6**, 2809–2811.

13 (*a*) H. Lv, L. Zhu, Y. Tang and J. Lu, *Appl. Organomet. Chem.*, 2014, **28**, 27–31; (*b*) H. Turkmena and I. Kani, *Appl. Organomet. Chem.*, 2013, **27**, 489–493; (*c*) R. Malacea, F. Chahdoura, M. Devillard, N. Saffon, M. Gomez and D. Bourissoua, *Adv. Synth. Catal.*, 2013, **355**, 2274–2284; (*d*) H. Kim, J. Lee, Y. Kim, Z. Zheng and S. W. Lee, *Eur. J. Inorg. Chem.*, 2013, 4958–4969; (*e*) X. Guo, Y. Wang, D. Wang, L. Cai, Z. Chen and X. Hou, *Dalton Trans.*, 2012, **41**, 14557–14567; (*f*) F. Godoy, C. Segarra, M. Poyatos and E. Peris, *Organometallics*, 2011, **30**, 684–688.

14 (*a*) S. Naik, M. Kumaravel, J. T. Magueb and M. S. Balakrishna, *Dalton Trans.*, 2014, **43**, 1082–1095; (*b*) S. Ramirez-Rave, F. Estudiante-Negrete, R. A. Toscano, S. Hernandez-Ortega, D. Morales-Morales and J. Grevy, *J. Organomet. Chem.*, 2014, **749**, 287–295; (*c*) H. Ren, Y. Xu, E. Jeanneau, I. Bonnamour, T. Tu and U. Darbost, *Tetrahedron*, 2014, **70**, 2829–2837; (*d*) P. Shah, M. D. Santana, J. García, J. L. Serrano, M. Naik, S. Pednekar and A. R. Kapdi, *Tetrahedron*, 2013, **69**, 1446–1453; (*e*) E. K. Bullough, M. A. Little and C. E. Willans, *Organometallics*, 2013, **32**, 570–577; (*f*) H. Yan, P. Chellan, T. Li, J. Maoa, K. Chibale and G. S. Smith, *Tetrahedron Lett.*, 2013, **54**, 154–157; (*g*) M. M. Tamizh, B. F. T. Cooper, C. L. B. Macdonald and R. Karvembu, *Inorg. Chim. Acta*, 2013, **394**, 391–400; (*h*) G. K. Rao, A. Kumar, B. Kumar, D. Kumar and A. Kumar Singh, *Dalton Trans.*, 2012, **41**, 1931–1937; (*i*) P. Mao, L. Yang, Y. Xiao, J. Yuan, X. Liu and M. Song, *J. Organomet. Chem.*, 2012, **705**, 39–43; (*j*) D. Pandiarajan and R. Ramesh, *J. Organomet. Chem.*, 2012, **708–709**, 18–24; (*k*) V. A. Kozlov, D. V. Aleksanyan, Y. V. Nelyubina, K. A. Lyssenko, P. V. Petrovskii, A. A. Vasilev and I. L. Odinets, *Organometallics*, 2011, **30**, 2920–2932.

15 T. E. Barder and S. L. Buchwald, *J. Am. Chem. Soc.*, 2007, **129**, 12003–12010.

Published on 18 June 2015. Downloaded by North Dakota State University on 08/07/2015 12:34:50.

16 (*a*) G. Zhang, X. Wang, C. Li and D. Yin, *Synth. Commun.*, 2013, **43**, 456–463; (*b*) X. D. Fei, Z. Zhou, W. Li, Y. M. Zhu and J. K. Shen, *Eur. J. Org. Chem.*, 2012, 3001–3008; (*c*) X. Hao, J. Yuan, G. A. Yu, M. Q. Qiu, N. F. She, Y. Sun, C. Zhao, S. L. Mao, J. Yin and S. H. Liu, *J. Organomet. Chem.*, 2012, **706–707**, 99–105; (*d*) S. Meiries, A. Chartoire, A. M. Z. Slawin and S. P. Nolan, *Organometallics*, 2012, **31**, 3402–3409.

17 L. Malatesta and M. Angoletta, *J. Chem. Soc.*, 1957, 1186–1188.

18 Yield has been calculated based on the amount of $Na_2[PdCl_4]$.

19 Chemical shifts for all NMR data are given in ppm and the multiplicity of the signals, along with the associated coupling constant(s), is given in parentheses. Overlapping signals are marked with an asterisk (*).

20 Yield has been calculated based on the amount of $[Pd_2(dba)_3]$.

21 G. M. Sheldrick, *SHELXS-97 and SHELXL-97, Fortran programs for crystal structure solution and refinement*, University of Gottingen, Gottingen, Germany, 1997.

22 M. Svensson, S. Humbel, R. D. J. Froese, T. Matsubara, S. Sieber and K. Morokuma, *J. Phys. Chem.*, 1996, **100**, 19357–19363.

 This journal is © The Royal Society of Chemistry 2015